Available online at www.sciencedirect.com
SCIENCE DIRECT®
Journal of Solid State Chemistry 178 (2005) 58–63
JOURNAL OF SOLID STATE CHEMISTRY
www.elsevier.com/locate/jssc

A green route for microwave synthesis of sodium tungsten bronzes Na_xWO_3 ($0<x<1$)

Juan Guo*, Cheng Dong, Lihong Yang, Guangcai Fu

National Laboratory for Superconductivity, Institute of Physics, Chinese Academy of Sciences, Zhongguancun South 3 Street, Haid, P.O. Box 603, Beijing 100080, People's Republic of China

Received 23 August 2004; received in revised form 8 October 2004; accepted 13 October 2004

Abstract

A green route has been developed for microwave synthesis of sodium tungsten bronzes Na_xWO_3 ($0<x<1$) from Na_2WO_4, WO_3 and tungsten powder. The hybrid microwave synthesis was carried out in argon atmosphere using CuO powder as the heating medium. Tungsten powder is used as the reducing agent instead of the alkali metal iodides previously used for the microwave synthesis of oxide bronzes. The prepared samples were characterized by powder X-ray diffraction, energy-dispersive X-ray analysis and scanning electron microscopy, and their phase constitutions, crystal structures and morphologies are in consistence with that in the literature. This synthesis method is simple, green and atom economic, and promising for preparation of other oxide bronzes and related compounds.

Keywords: Microwave heating; Sodium tungsten bronzes; Green synthesis; Atom economic reactions

1. Introduction

Tungsten bronzes are a group of nonstoichiometric compounds with the general formula of M_xWO_3, where x is in the range of $0<x<1$ and M is a metal element. The structure of tungsten bronzes (M_xWO_3) consists of regular or distorted corner-sharing WO_6 octahedra, and the metal atom M is intercalated into the WO_6 network. In the past years, they have received intensive attention due to their unusual physical and chemical properties. An enormous amount of data was accumulated on their crystal structure [1–3], electronic and magnetic properties [4,5], and superconductivity [6–16]. Tungsten bronzes have been found technological applications such as in electrochromic devices, humidity sensors, solid fuel cells, secondary batteries, ion sensitive electrodes, etc. [17–19].

Among all kinds of tungsten bronzes known, the sodium tungsten bronzes are the best studied ones ever since their discovery in 1823 [20], and their physical properties and structures are strongly dependent on their compositions. For example, $Na_{0.025}WO_3$ is semiconducting [4], while Na_xWO_3 is metallic when $x>0.58$ [21,22]. The superconductivity of sodium tungsten bronzes is also an attractive topic [6,7]; especially, the possibility of superconductivity with T_c around 91 K in WO_3 crystals with a surface composition of $Na_{0.05}WO_3$ [8,9] has been given remarkable notice recently [10–12,23]. The colors of the Na_xWO_3 crystals change from golden yellow through red and violet to dark blue as x decreases from 1 to 0.1 [24], which can be explained using a $5d(t_{2g})$-band model [4]. The phase diagrams in the Na_xWO_3 system have been systemically studied in 1950s [1]. From $x=0$ to 0.1 three phases appear in the order of monoclinic, orthorhombic and tetragonal I. Between $x=0.11$ and 0.28, two tetragonal phases coexist and tetragonal II has a range of homogeneity from $x=0.28$ to 0.38. For $0.39<x<0.43$, tetragonal II

*Corresponding author. Fax: +86 10 8264 9531.
E-mail address: guojuan@ssc.iphy.ac.cn (J. Guo).

0022-4596/$ - see front matter © 2004 Elsevier Inc. All rights reserved.
doi:10.1016/j.jssc.2004.10.017

and cubic phases coexist. This is followed by a cubic phase in the range of $x = 0.44$–0.95. The tetragonal I and II phases have approximately the same lattice parameter c ($c \approx a_0$, a_0 is the lattice parameter for the basic perovskite structure), but they have distinct lattice parameter a ($a \approx \sqrt{2}a_0$ for the former and $a \approx 3a_0$ for the latter). In the following content, the tetragonal I and the tetragonal II phases are labeled as TET I and TET II, respectively, for brevity.

Various syntheses techniques, such as high-temperature electrolysis and reduction [2,6–8], were developed to prepare sodium tungsten bronzes. Some low-temperature methods, such as sol–gel, co-precipitation and solvothermal syntheses [25–27] have also been employed. In addition, nanocrystalline powders of sodium tungsten bronzes can be obtained by mechanochemical synthesis [23].

In recent years, the microwave processing has been used extensively for material synthesis, because it is clean, time saving and energy efficient [28]. Many inorganic materials, such as binary compounds [29–31], superconductors [32–36], and other materials [37] have been synthesized using the microwave methods. The pioneer research on microwave synthesis of oxide bronzes was reported by Rao et al., and they have obtained A_xWO_3, A_xMoO_3 and $A_xV_2O_5$ (A = K, Li, Cu) [38] from metal oxides and alkali metal iodides. The advantages of their method are low reaction temperatures and fast reaction rates. However, iodine gas in the products possibly pollutes the environment, and will be lost if it is not reclaimed. In addition, they did not report the synthesis of sodium tungsten bronzes. In the present study, we tried to improve Rao's procedure so that the synthesis was both green and atom economic. Therefore, we used tungsten powder instead of alkali metal iodides as reducing agent. Furthermore, hybrid heating was applied in order to accelerate the reaction rates.

2. Experimental

Analytically pure $Na_2WO_4 \cdot 2H_2O$, WO_3 and W powders were used as starting materials. They were mixed by mole ratio according to the following reaction equation:

$$\frac{x}{2}Na_2WO_4 + \frac{3-2x}{3}WO_3 + \frac{x}{6}W = Na_xWO_3. \quad (1)$$

The mixed powder was finely ground and then pressed into pellets ($\Phi 20 \times 3$ mm) with a pressure of 8 MPa. The reactant pellet was placed in a small alumina crucible. The pellet was surrounded by the mixed reactant powder and then covered by thermal insulation materials to reduce the heat dissipation. The small crucible was placed in the middle of another large alumina crucible filled with CuO powder. The CuO powder was used as a heating medium because CuO could absorb microwave radiation very effectively [35]. The microwave heating was carried out in flowing Ar gas. The inlet of argon gas was an Al_2O_3 tube drilling through the crucible lid, and the Ar gas outlet was the narrow gaps between the crucible and the lid. The schematic illustration of microwave reactor is shown in Fig. 1. The reactor was placed in a modified domestic microwave oven (KE23B-W, Midea, China) working at the frequency of 2.45 GHz and maximum power of 800 W. The duration of microwave heating was 13–15 min. The samples were cooled to room temperature in flowing argon.

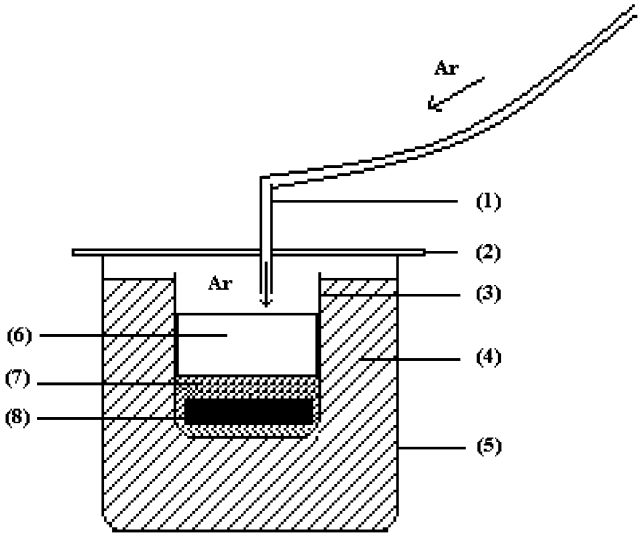

Fig. 1. Schematic illustration of microwave heating setup: (1) Al_2O_3 tube, (2) Al_2O_3 pellet, (3) small crucible, (4) CuO powder, (5) large crucible, (6) thermal insulation material, (7) reactants powder, and (8) reactants pellet.

The prepared samples were characterized by powder X-ray diffraction (XRD), energy-dispersive X-ray analysis (EDX) and scanning electron microscopy (SEM). The powder X-ray diffraction data was obtained using an M18X-AHF rotating-anode diffractometer with Cu$K\alpha$ radiation. Lattice parameters were calculated using the least-square method with PowderX program [39]. The chemical compositions, the grain morphology and microstructure were performed using a scanning electron microscope (XL30 S-FEG).

3. Results and discussion

The preparation conditions and the XRD and EDX analysis results for all samples are listed in Table 1. The microwave heating time is less than 15 min, which is much shorter than that used in the conventional synthesis. Therefore, the loss of sodium during microwave heating is negligible. For example, the loss of sodium for the sodium-rich samples with $x = 0.8$ and 0.5

Table 1
Sodium tungsten bronzes Na_xWO_3 prepared by microwave heating method

Composition (x)		Microwave heating time (min)	Color	Crystal structure	a (Å)	c (Å)
Nominal	EDX result					
0.8	0.794	15	Yellow	Cubic (single phase)	3.8468(1)	
0.5	0.491	14	Purple	Cubic (single phase)	3.8230(1)	
0.4	0.375	15	Blue	TET II (single phase)	12.0955(7)	3.7526(2)
0.3	0.285	14	Blue	TET II (single phase)	12.0826(7)	3.7520(2)
0.2	0.172	15	Blue	TET II + TET I (two phases)	12.0774(5)	3.7530(2)
					5.2565(4)	3.9003(3)
0.1	0.096	14	Dark blue	TET I (single phase)	5.2550(4)	3.9002(3)
0.05	0.090	13.5	Dark blue	TET I (Major), WO_3 (minor)	5.2453(6)[a]	3.8777(4)[a]

[a] a and c are cell parameters of TET I (major) for $Na_{0.05}WO_3$.

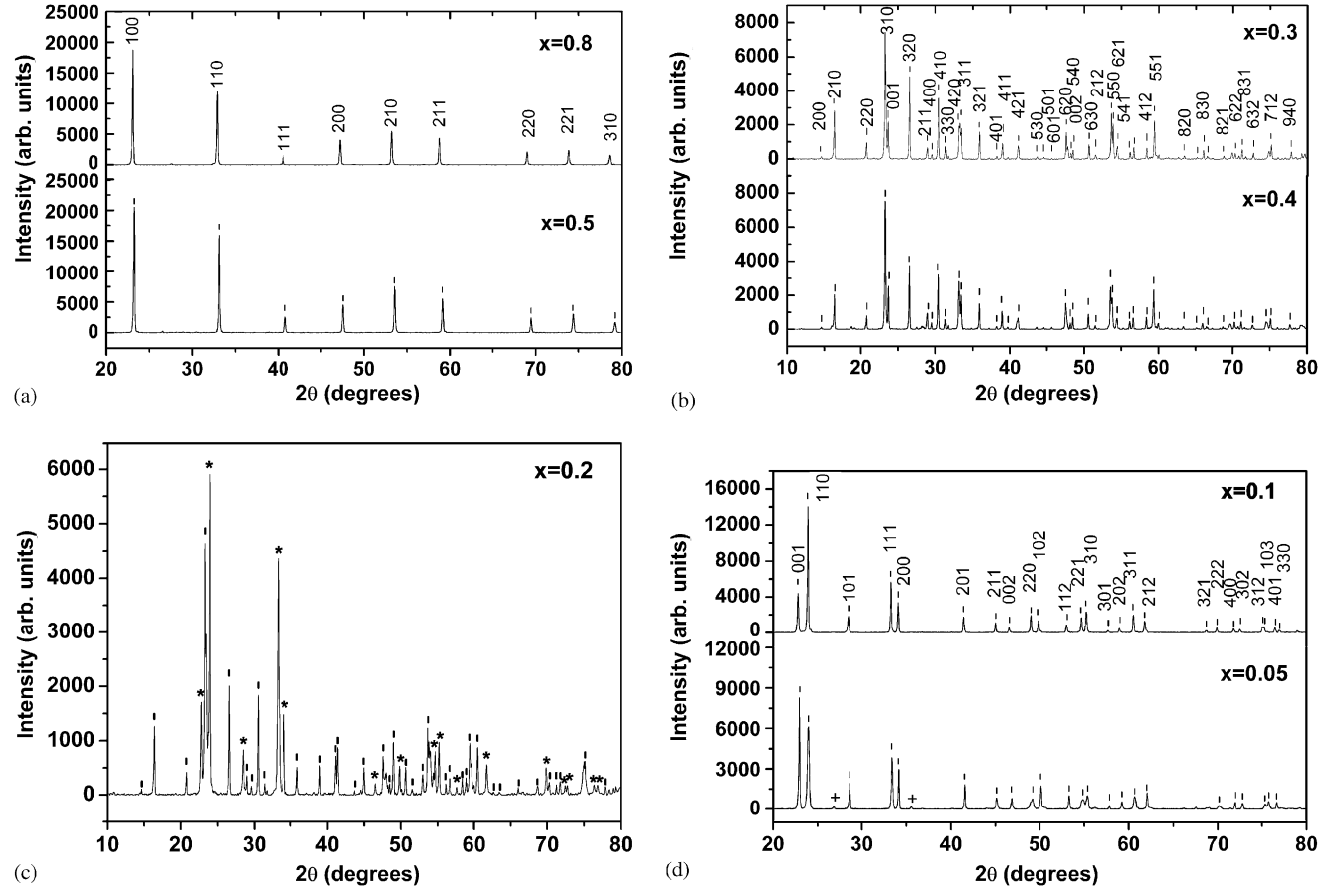

Fig. 2. XRD patterns of sodium tungsten bronzes Na_xWO_3 prepared by microwave heating method. (a) Cubic structure for $x=0.5$, 0.8. (b) Tetragonal II structure for $x=0.3$, 0.4. (c) Two phases tetragonal I (*) and II (|) structure for $x=0.2$. (d) Tetragonal I structure for $x=0.1$, 0.05, the peaks of WO_3 impurity are marked +.

is less than 1% and 2%, respectively. The composition variations are no more than 6% except the biphasic samples with $x=0.05$ and 0.2. Large composition deviations for these biphasic samples can be attributed to the phase segregation evidenced by the XRD and SEM analysis, and further explanation will be given in the following context.

The XRD patterns of Na_xWO_3 ($0<x<1$) samples prepared by the hybrid microwave method are shown in Fig. 2. Diffraction peaks in these patterns are quite sharp indicating that the samples are well crystallized. All samples are single phase except the samples with $x=0.05$ and 0.2, and these results are consistent with the phase diagram for Na_xWO_3 [1]. The samples

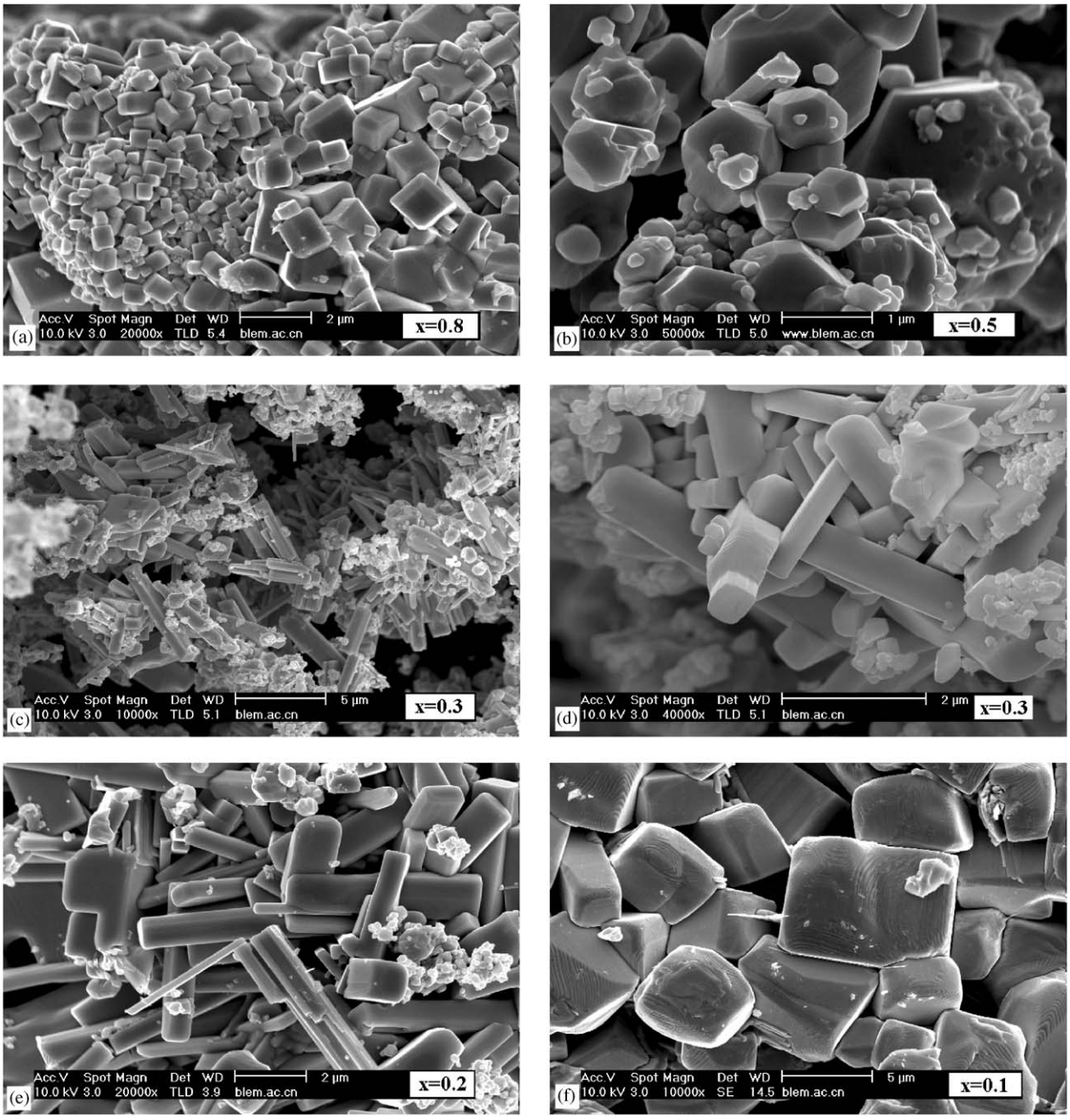

Fig. 3. SEM micrographs of sodium tungsten bronzes Na_xWO_3 prepared by microwave heating method. (a) $x=0.8$. (b) $x=0.5$. (c) and (d) $x=0.3$. (e) $x=0.2$. (f) $x=0.1$.

with $x \geqslant 0.5$ form cubic phase and samples with x in the range from 0.1 to 0.5 form tetragonal phases. As it is shown in Fig. 2b and d, single phase TET II and TET I are formed for samples with $x=0.3$ and $x=0.1$ respectively; two phases TET I and TET II structure coexist in sample $Na_{0.2}WO_3$ (Fig. 2c). The major phase in the sample with $x=0.05$ is TET I with minor WO_3 (Fig. 2d). According to these results, the large composition deviations for sample with $x=0.05$ and 0.2 can be explained as follows. There are two phases (TET I and TET II) with different sodium content in sample $Na_{0.2}WO_3$. Therefore, inhomogenous distribution of these two phases can cause the composition deviation in the EDX analysis. Similarly, the surface segregation of sodium-rich phase is a possible reason for the composition deviation for the $x=0.05$ sample. In addition, the relative error of the sodium content is high for low-sodium sample in the EDX measurement. When $x=0.4$, two phases TET II and cubic coexist in the phase diagram. However, the actual composition of sample

$Na_{0.4}WO_3$ is 0.375 and falls into the single phase (TET II) region ($0.28 < x < 0.39$). As a result, this sample is a single phase.

The scanning electron microscopy (SEM) images of the samples are shown in Fig. 3. Crystallites with cubic, truncated octahedron and rectangular morphology are clearly visible in the images. It can be seen that the crystallite shape changes with the sodium content for cubic phase tungsten bronzes. For sample with $x = 0.8$, the edge length of cubic crystallites is in the range of 0.2–2 μm (Fig. 3a) and crystal facets are distinguishable. The crystal shape of the $Na_{0.5}WO_3$ is truncated octahedron (Fig. 3b), which is different from that of $Na_{0.8}WO_3$. The diagonal dimension of the larger truncated octahedra is between 2 and 3 μm, whereas the height varies from 1 to 2 μm. Although the outline of crystallites is not identical, most of them are irregular truncated octahedrons and the shape of hexagonal facets is similar. For $Na_{0.3}WO_3$, long rectangular crystallites are present (Fig. 3c and 3d). The edge length of their basal planes varies from 0.5 to 1 μm, whereas their length is between 2 and 5 μm. The crystallite morphology of the biphasic sample with $x = 0.2$ is also rectangular (Fig. 3e) similar to that of the sample $Na_{0.3}WO_3$, and growing short rectangular crystallites are detected besides slender ones assigned to the TET II phase. The short crystallites are typical for the TET I phase and their number is very small relative to the amount of long ones. For sample $Na_{0.1}WO_3$ (Fig. 3f), irregular and stubby rectangular crystallites can be seen. The length of large ones is up to some 7 μm. There are growth terraces on the crystal facets of some crystallites (see Fig. 3f and d).

From Table 1, it can be seen that the colors of the Na_xWO_3 samples gradually change from dark blue to yellow with the increase of x. This variation of colors also agrees with that reported previously [24].

In the present study, tungsten powder instead of alkali metal iodides was used as reducing agent in the microwave synthesis of oxide bronzes. This improvement makes the synthesis route green and atom economic. It is green because the pollution of iodine is avoided, and it is atom economic because all atoms in the reactants are retained in the final product Na_xWO_3. In addition, our hybrid microwave-heating route can be used in bronze synthesis where the reactants are not easily heated by the microwave. The starting mixture of $Na_2WO_4 \cdot 2H_2O$, WO_3 and W powder are poor susceptors of microwave; therefore the reaction temperature is hardly attained without the heating medium. In our experiments, the crucible can be heated to red hot in about 7 min.

Finally, we would like to discuss on the possible reason for the enhanced reaction rate in the hybrid microwave synthesis. The reaction mechanism in the microwave synthesis of the tungsten bronzes is similar to that in the conventional solid-state reactions. It involves the oxidation of the tungsten metal and then the sodium ions intercalate into the network of W–O octahedra by thermal diffusion. At the initial stage, the microwave radiation is mainly absorbed by the CuO powder and its temperature increases very quickly. Subsequently, the samples are heated by the hot heating medium. Although the starting materials are not good microwave absorber at room temperature, they can absorb the microwave radiation more effectively when they are hot. Therefore, the reaction rate can be significantly accelerated, and the tungsten bronzes can be obtained within several minutes.

4. Conclusion

Sodium tungsten bronzes Na_xWO_3 ($0 < x < 1$) have been prepared by a hybrid microwave synthesis using CuO powder as the heating medium. The tungsten powder instead of alkali metal iodides was used as reducing agent. The chemical composition, phase constitution, crystal structure and morphology of the obtained samples were characterized by energy-dispersive X-ray analysis, X-ray diffraction and scanning electron microscopy; and the results were in consistence with that reported previously. The prepared samples have the potential for various applications. This route avoids the pollution of iodine gas, so it is green as well as atom economic. In addition, it is simpler and faster than most previous methods. This hybrid microwave route is promising for the synthesis of other oxide bronzes when the reactants are poor microwave absorbers.

Acknowledgment

This work was supported by the Ministry of Science and Technology of China (NKBRSF-G 19990646) and the National Natural Science Foundation of China (No. 20141002 and No. 20271052).

References

[1] A.S. Ribnick, B. Post, E. Banks, in: R. Ward (Ed.), Nonstoichiometric Compounds, American Chemical Society, Washington, 1963, pp. 246–253 and references therein.
[2] H.R. Shanks, J. Crystal Growth 13/14 (1972) 433.
[3] S.T. Triantafyllou, P.C. Christidis, Ch.B. Lioutas, J. Solid State Chem. 133 (1997) 479.
[4] M.J. Sienko, in: R. Ward (Ed.), Nonstoichiometric compounds, American Chemical Society, Washington, 1963, pp. 224–236 and references therein;
H.R. Shanks, P.H. Sidles, G.C. Danielson, in: R. Ward (Ed.), Nonstoichiometric compounds, American Chemical Society, Washington, 1963, pp. 237–245 and references therein.
[5] M.J. Sienko, S.M. Morehouse, Inorganic Chem. 2 (1963) 485.
[6] Ch.J. Raub, A.R. Sweedler, M.A. Jensen, S. Broadston, B.T. Matthias, Phys. Rev. Lett. 13 (1964) 746.

[7] H.R. Shanks, Solid State Commun. 15 (1974) 753.
[8] S. Reich, Y. Tsabba, Eur. Phys. J. B 9 (1999) 1.
[9] A. Shengelaya, S. Reich, Y. Tsabba, K.A. Müller, Eur. Phys. J. B 12 (1999) 13.
[10] N.N. Garif'yanov, E.L. Vavilova, Physica C 383 (2003) 417.
[11] R. Brusetti, P. Haen, J. Marcus, Phys. Rev. B 65 (2002) 144528.
[12] G. Leitus, H. Cohen, S. Reich, Physica C 371 (2002) 321.
[13] L.H. Cadwell, R.C. Morris, W.G. Moulton, Phys. Rev. B 23 (1981) 2219.
[14] R.K. Stanley, R.C. Morris, W.G. Moulton, Phys. Rev. B 20 (1979) 1903.
[15] M.R. Skokan, W.G. Moulton, R.C. Morris, Phys. Rev. B 20 (9) (1979) 3670.
[16] A.R. Sweedler, J.K. Hulm, B.T. Matthias, T.H. Geballe, Phys. Lett. 19 (1965) 82.
[17] C.G. Granqvist, Hand Book of Inorganic Electrochromic Materials, Elsevier, Amsterdam, 1995 and references therein.
[18] I. Tsuyumoto, T. Kudo, Sensors Actuators B Chemical 30 (1996) 95.
[19] P.R. Slater, J.T.S. Irvine, Solid State Ionics 124 (1999) 61.
[20] F. Wöhler, Ann. Chim. Phys. 43 (1823) 29.
[21] W. Macneill, Ph.D. Thesis, Temple Univ., 1961.
[22] W.R. Gardner, G.C. Danielson, Phys. Rev. 93 (1954) 46.
[23] J.H. Wang, G.Q. Liu, Y.W. Du, Mater. Lett. 57 (2003) 3648.
[24] J.K. Liang, Crystal Structure Determination Using Powder Diffraction Method Part I, Science Press, Bei Jing, 2003 p 232 (in Chinese).
[25] X.Z. Zhao, R. Roy, K.A. Cherian, A. Badzian, Nature 385 (1993) 513.
[26] Q.W. Chen, Y.T. Qian, Physica C 224 (1994) 283.
[27] Y.D. Li, X.F. Duan, J. Chem. Soc. 119 (1997) 7869.
[28] D.K. Agrawal, Curr. Opin. Solid State Mater. Sci. 3 (1998) 480.
[29] R.D. Ramesh, B. Vaidhyanathan, M. Ganguli, K.J. Rao, J. Mater. Res. 2 (1994) 3025.
[30] B. Vaidhyanathan, M. Ganguli, K.J. Rao, Mater. Res. Bull. 30 (1995) 1173.
[31] B. Vaidhyanathan, K.J. Rao, J. Mater. Res. 12 (1997) 1.
[32] M. Kato, K. Sakakibara, Y. Koike, Jpn. J. Appl. Phys. 36 (1997) L1291.
[33] M. Kato, K. Sakakibara, Y. Koike, Appl. Supercond. 5 (1997) 33.
[34] M. Kato, K. Sakakibara, Y. Koike, Jpn. J. Appl. Phys. 38 (1999) 5867.
[35] D.R. Baghurst, A.M. Chippindale, D.M.P. Mingos, Nature 332 (1988) 311.
[36] S.S. Bayya, R.L. Snyder, Physica C 225 (1994) 83.
[37] Y.F. Liu, X.Q. Liu, G.Y. Meng, Mater. Lett. 48 (2001) 176.
[38] K.J. Rao, P.A. Ramakrishnan, R. Gadagkar, J. Solid State Chem. 148 (1999) 100.
[39] C. Dong, J. Appl. Cryst. 32 (1999) 838.